Genetics and Genomics

Mitochondrial adenine base editing of mouse somatic tissues via adeno-associated viral delivery

Reviewed Preprint
v1 • March 4, 2025
Not revised

Christian D Mutti, Lindsey Van Haute, Lucia Luengo-Gutierrez, Keira Turner, Pedro Silva-Pinheiro, Michal Minczuk

MRC Mitochondrial Biology Unit, University of Cambridge, Cambridge, United Kingdom • Department of Clinical Neurosciences, University of Cambridge, Cambridge, United Kingdom

eLife Assessment

The authors have demonstrated the use of adenine base editors delivered via adeno-associated viruses to introduce edits in the mitochondrial genome. The manuscript describes the methodology well, and the conclusions are **convincingly** supported by the results. The **valuable** results highlight the potential of these base editors to model mtDNA variations in somatic tissues in animal models.

https://doi.org/10.7554/eLife.105080.1.sa2

Abstract

The development of adenine base editing in mitochondria, alongside cytidine base editing, has significantly expanded the genome engineering capabilities of the mitochondrial DNA. We tested the recent advancements in adenine base editing technology using optimised TALEs targeting genes *Mt-Cytb*, *Mt-CoII* and *Mt-Atp6* in mouse cells, and observed successful A:T to G:C conversions within the target windows of each gene. Then, we used the best performing pairs targeting the *Mt-Atp6* gene to inject mice using adeno-associated viral delivery to post-mitotic tissue. We observed limited efficiency of adenine edits in mouse somatic tissue after 4 weeks, suggesting the necessity of further optimisation of this technology.

Introduction

Mitochondria, essential organelles responsible for energy production and cellular homeostasis, possess their own genome distinct from the nuclear one. Mitochondrial DNA (mtDNA) alterations have been implicated in various human diseases, making precise genome editing tools invaluable for both basic research and potential therapeutic interventions [1]. Base editing has emerged as a transformative technology for precise genome manipulation, offering unprecedented

capabilities for targeted nucleotide alterations without inducing double-strand breaks. While extensively explored in the nuclear genome, the application of base editing to mtDNA presents unique opportunities, but also challenges [2].

The inability to efficiently deliver nucleic acids into mitochondria has prompted the development of genome modification technologies based on custom DNA-binding protein. These technologies included mitochondrially-targeted zinc finger nucleases (mtZFNs), transcription activator-like effector nucleases (mitoTALEs) and meganuclease (mitoARCUS) and have been used for site-specific cleavage of mtDNA [3], [4], [5], [6], [7]. Combining ZF or TALE programmable DNA-binding proteins with deaminase enzymes, such as cytidine or adenine deaminases, allows for C:G to T:A or A:T to G:C conversions, respectively. The first major breakthrough was DddA-derived cytosine base editors (DdCBEs) which allowed for site-specific C:G to T:A mutations in the mtDNA for the first time [8]. The initial dimeric DdCBE architecture contained the catalytic domain of DddAtox bacterial cytidine deaminase acting on double-stranded DNA, split into two inactive fragments (at positions G1333 or C1397), which were brought together by TALE DNA binding domains [8]. The technology was rapidly used by our lab and others for many applications including; knocking out each mtDNA-encoded protein-coding gene [9], reverse genetics approaches [10] and *in vivo* applications in zebrafish[11], [12], rats [13] and mice [14], [15]. The technology was also evolved to improve efficiency and widen compatibility for different sequence contexts and DNA-binding proteins[16], [17], [18], [19], [20]. The discovery of mitochondrial cytidine base editing provided foundation for the development of adenine base editors in mitochondria using the TadA8e enzyme, deemed transcription-activator-like effector (TALE)-linked deaminases (TALEDs), majorly increasing the capabilities of the mitochondrial gene editing toolkit [21]. Further developments included adenine editors containing a nickase to generate the single-stranded DNA required for deaminase activity (mitoBEs) [22]. In this study, we sought to apply the adenine base editing technologies, TALEDs and mitoBEs, *in vivo* using adeno-associated viral delivery to mouse somatic tissues.

Materials and methods

Plasmid construction and viral vectors

The TALE sequences and plasmids used were designed as reported in [9]. To construct the plasmids used in the cell screen, the functional domain was changed to varying architectures of TadA8e, DddAtox(E1347A) or BspD61(C) using AvrII and XbaI for pTracer or BamHI and KpnI for pcDNA3.1. Vector construction intended for AAV production was achieved by restriction digest of the transgenes using 5' NotI and 3' BamHI sites, allowing cloning into a rAAV2-CMV backbone, previously reported in [15]. The cloned plasmids were used to generate recombinant AAV9 viral particles at the UNC Gene Therapy Center, Vector Core Facility (Chapel Hill, NC) and VectorBuilder.

Cell culture and transfections

NIH/3T3 cells (CRL-1658TM, obtained from the American Type Culture Collection (ATCC)) were maintained at 37 °C in a 5% (vol/vol) CO2 atmosphere in complete Dulbecco's Modified Eagle Medium (DMEM) containing 4.5 g/L glucose, 2 mM glutamine, and 110 mg/ml sodium pyruvate, supplemented with 10% calf bovine serum with iron and 5% penicillin/streptomycin (all sourced from Gibco). Regular mycoplasma tests performed on the culture medium yielded negative results.

For the adenine base editor pair screening, NIH/3T3 mouse cells were seeded in six-well tissue culture plates at a 70% confluency and transfected with 3200 ng of each monomer (L and H), using 16 µl of FuGENE-HD (Promega) according to the manufacturer's instructions. After 24 h, the cells were harvested for Fluorescence-activated cell sorting (FACS) and sorted for GFP and mCherry double-positive cells employing a BD FACSMelody^{TM} Cell sorter. The collected double-positive cells were allowed to recover for an additional 6 days before being utilised for DNA extraction, as

detailed below. For cell survival experiments, AAV plasmids were transfected with empty GFP plasmid in a 1:1 ratio, sorted using BD FACSMelody^{TM} Cell sorter and replate for 3 days. Cells were then analysed using Countess™ 3 Automated Cell Counter (Invitrogen) to determine cell survival.

Animals

(Ethics statement) All animal experiments were approved by the local Animal Welfare Ethical Review Body (AWERB) at the University of Cambridge and carried out in accordance with the UK Animals (Scientific Procedures) Act 1986 (Procedure Project Licence: PP1740969) and EU Directive 2010/63/EU). Mice on C57BL/6J background were sourced from Charles River Laboratories. Animals were housed in a temperature- and humidity-controlled environment, maintained under a 12-hour light/12-hour dark cycle, and continuous access to food and water *ad libitum*. Euthanasia was carried out via cervical dislocation. Newborn pups [both males and females on Postnatal day 1(P1)] were injected with a dose of 5×10^{11} vg per monomer per animal (1×10^{12} vg total) via the temporal vein (systemic administration), using a 30 G, 30° bevelled needle syringe. Control P1 pups were injected with equivalent volumes of vehicle buffer (1× PBS, 230 mM NaCl, and 5% w/v D-sorbitol). A total of 3 animals per group were used.

Genomic DNA isolation and Sanger sequencing

NIH/3T3 mouse cells underwent trypsinisation for collection, followed by a single wash in PBS and extraction using the DNeasy Blood & Tissue Kit (QIAGEN) following manufacturers guidelines. The lysates were then extracted using DNeasy Blood & Tissue Kit (QIAGEN) following manufacturers guidelines. Genomic DNA extraction from mouse samples was also extracted using the DNeasy Blood & Tissue Kit (QIAGEN) following manufacturers guidelines. For Sanger sequencing, the edited region underwent PCR amplification using GoTaq G2 DNA polymerase (Promega) and using primers and PCR protocol for each site as listed in [9]. PCR purification and subsequent Sanger sequencing were conducted by GENEWIZ/AZENTA (UK).

High-throughput targeted amplicon mtDNA sequencing, processing and mapping

mtDNA-wide sequence analysis was performed, sequenced and analysed as in [9]. Briefly, two overlapping long amplicons (8,331 bp and 8,605 bp) spanning the entire mtDNA molecule were generated via long-range PCR utilising PrimeSTAR GXL DNA polymerase (TAKARA). Tagmentation and indexing PCR were performed using the Nextera XT index kit (Illumina, FC-131-1096) as per the manufacturer's instructions. Subsequently, libraries were subjected to high-throughput sequencing on the Illumina NovaSeq platform (PE250), with demultiplexing performed using the respective manufacturer's software.

For processing and mapping of the high-throughput data related to mtDNA-wide analysis, sequenced reads underwent quality trimming and 3' end adaptor clipping simultaneously using Trim Galore! (--paired). Reads were aligned to ChrM of the mouse reference genome (GRCm39) with Bowtie2 (--very-sensitive; --no-mixed; --no-discordant). Count tables were then generated using samtools mpileup (-q 30) and varscan.

Quantification of viral genomes copy number and relative mtDNA content by quantitative real-time PCR

Quantitative real-time PCR analyses were conducted in a QuantStudioTM 3 system (Thermo Fisher) using TaqMan™ Gene Expression Master Mix (Thermo Fisher), following the manufactureŕs instructions, and Ct values were obtained using the system's built-in software. Each reaction was performed in a final volume of 20 µl in technical triplicates, with each dataset representing samples from an individual mouse.

To assess the relative mtDNA content in mouse tissue samples, mtDNA levels were quantified using primers and probes targeting MT-ND1: Mmu_Nd1_Fw: 5'-GAG CCT CAA ACT CCA AAT ACT CAC T −3'; Mmu_Nd1_Rv: 5'-GAA CTG ATA AAA GGA TAA TAG CTA TGG TTA CTT CA −3'; Mmu_Nd1_probe: 5'-/56-FAM/ CCG TAG CCC /ZEN/ AAA CAA T /3IABkFQ / −3'. MT-ND1 levels were normalized to the nuclear gene Actin using the following primers and probe: Mmu_Actin_Fw: 5'-CTG CTC TTT CCC AGA CGA GG −3'; Mmu_Actin_Rv: 5'-AAG GCC ACT TAT CAC CAG CC −3'; Mmu_Actin_probe: 5'-/56-TAMN/ ATT GCC TTT CTG ACT AGG TG /3BHQ/ −3'. ΔΔCt analysis was employed to calculate the relative mtDNA copy number, with vehicle-injected mice serving as the control.

Immunoblotting of adenine base editors in mouse tissues

Mouse tissue samples (~50 mg) underwent homogenization in 200 uL of ice-cold RIPA buffer (consisting of 150 mM NaCl, 1.0% NP-40, 0.5% sodium deoxycholate, 0.1% SDS, and 50 mM Tris, pH 8.0) supplemented with 1X cOmplete™ mini EDTA-free Protease Inhibitor Cocktail (Roche, UK), utilizing a gentleMACS™ dissociator. Following homogenization, the samples were incubated on ice for 20 mins and then clarified by centrifugation (20,000 × g for 20 min at 4 °C). Protein lysates (~20 µg) were combined with 10 X NuPAGE™ sample reducing agent and 4X NuPAGE™ LDS sample buffer (Invitrogen), followed by incubation for 5 min at 95 °C. The denatured protein samples were subsequently separated in a Bolt 4–12% Bis-Tris pre-cast gel (Thermo Fisher) and transferred onto a PVDF membrane using an iBlot 2 gel transfer system (Thermo Fisher), following the manufacturer's guidelines. Residual proteins remaining in the gel were visualized using SimpleBlue SafeStain (Thermo Fisher) and served as a loading control. The membrane was blocked in 5% milk in PBS with 0.1% Tween 20 (PBS-T) for 1 h at room temperature (RT) before being probed with either rat anti-HA-tag antibody (Roche, 11867423001) diluted 1:1000 in 5% milk in PBST, mouse anti-FLAG-M2-tag antibody (Sigma–Aldrich, F3165) diluted 1:2000 in 5% milk in PBST or mouse OXPHOS cocktail (abcam, ab110412) diluted 1:300 in 5% milk in PBST. After three washes with PBS-T for 10 min each at RT, the membranes were incubated with HRP-linked secondary antibodies, either anti-rat IgG (Cell Signaling, 7077 S) or anti-mouse IgG (Promega, W4021), diluted 1:5000 in 5% milk in PBST. Following another three washes as before, the membranes were digitally imaged using an Amersham Imager 680 blot and gel imager (GE Healthcare) upon exposure to Amersham ECLTM Western Blotting Detection Reagents (GE Healthcare).

Results and discussion

Adenine base editing *in vitro*

The originally reported adenine base editors (TALEDs) were shown to work within varying efficacies dependent on the architecture used [21]. The authors used either: (1) dimeric TALEDs (dTALED), which combines two sequence specific TALE arrays binding to opposite strands, with either the catalytically inactive (E1357A) DddAtox or TadA8e at their C-terminus, (2) split DddA TALED (sTALED) which uses the dimeric approach but with the DddAtox(E1357A) split at the G1397 position or (3) monomeric TALED (mTALED) which uses a single TALE-array attached to both the DddAtox(E1357A) and the TadA8e adenine deaminase (**Fig. 1a**; **Supplementary Fig. 1**). In order to test the efficiency of the TALED technology, we used validated TALE arrays for mtDNA-encoded mouse *Mt-Cytb*, *Mt-CoII* and *Mt-Atp6* from our previous work [9]. These TALEs are all known to bind the desired mtDNA position and induce high levels of cytosine base edits, and therefore acted as a good starting point to test the adenine base editing technology *in vitro*. Each of the TALE pair was cloned into plasmids containing the different DddAtox(E1357A)/TadA8e variations. This resulted in a total of 6 combinations which were transfected into WT NIH-3T3 mouse cells, sorted and replated to grow for 6 days. The levels of detectable editing from Sanger sequencing varied significantly (**Supplementary Figs. 2**-**4**), which was quantified using next generation sequencing (NGS) (**Fig. 1b**). For *Mt-Cytb*, low editing levels were observed in one of

the dimeric DddAtox(E1357A) and TadA8e combinations, and also for the monomeric H strand binding construct (**Fig. 1b**). In the case of *Mt-CoII*, the dimeric DddAtox and TadA8e version showed editing alongside the split DddAtox(E1357A) dimeric combination (**Fig. 1b**). Finally, *Mt-Atp6* showed similar editing in both dimeric, split DddAtox(E1357A) and monomeric architectures (**Fig. 1b**). The highest editing efficiency we achieved after 7 days in vitro was 17%, comparable to previous reports for mouse NIH-3T3 cells, albeit lower than that observed in human cell A-to-G editing. [21], [22], [23]. In the cases where editing was observed, it was present at multiple A:T sites within/across the editing window rather than being specific to predominantly one position as with the DdCBE technology [9]. The NGS analysis also allowed for mtDNA-wide off-target editing frequency to be calculated. The off-target editing was approximately 0.1% for all constructs which falls within the variation in unedited WT cells (**Fig. 1c**), suggesting generally lower activity of TALEDs, as compared to DdCBEs [9]. The off-targets for these constructs are therefore not concerning, although the on-target levels are relatively low and if they increased, the off-targets would likely follow.

We next decided to focus on *Mt-Atp6*, as we previously successfully edited this gene *in vitro* and *in vivo* using cytosine base editors [9]. We tested the strand selective mitochondrial base editors (mitoBEs), which use nickase enzymes to create the single stranded DNA required for TadA8e activity (**Fig. 2a**, **Supplementary Fig. 1**) [22]. We used the Nt.BspD61(C) nickase due to its lack of sequence specificity, unlike the MutH* nickase used in the previous study, which requires a 5'-GAT-3' sequence not present in the *Mt-Atp6* target window. Following the NIH-3T3 cells transfection and selection (see above), the NGS analysis revealed up to 4% editing at multiple sites withing the targeting window between the TALE biding sites when using the mitoBEs (**Fig. 2b**, **Supplementary Fig. 5**), whilst mtDNA-wide off-targets were not significantly above control levels (**Fig. 2c**). Taken together, our study replicated the outcomes documented for both TALEDs and mitoBEs, with the efficiencies and editing patterns observed in mouse cells being largely consistent with those reported previously [21], [22], [23].

Adenine base editing *in vivo*

Next, we intended to investigate if adenine base editing could be used to edit mtDNA in the post-mitotic tissues of neonate mice, as reported by us previously for various cytosine editors [15], [16]. Informed by our *in vitro* data, we decided to test the best performing *Mt-Atp6* constructs in dimeric architecture using TadA8e with the H-strand binding TALE and either the inactive DddAtox(E1357A) (the TALED architecture) or nickase Nt.BspD61(C) (the mitoBE architecture) with the L-strand binding TALE. We cloned the respective DNA sequences in a AAV-compatible vector and proceeded with encapsidation according to our standard AAV production approach [15], [24]. However the titres for the H-strand TadA8e construct were approximately 1000-fold lower than for the L-strand DddAtox(E1357A) or L Nt.BspD61(C), which proved insufficient for any mouse injections. We repeated the procedure at two different facilities with similar results. During the course of these experiments a study was published addressing the significant RNA off-targets of the TadA8e enzyme greatly affecting cell viability upon transfection, therefore, we hypothesized that this was likely the reason for the failure to produce AAVs containing the TadA8e enzyme [23]. The study engineered the TadA8e protein to reduce RNA off-target edits, with the V28R mutation preventing >99% RNA-induced off-targeting and leading to increased cell viability [23]. We installed the V28R mutation into the TadA8e AAV plasmid and tested the effect of TadA8e(V28R) on cells following transfection of HEK293T and comparing it to the unmodified TadA8e AAV plasmid. Consistent with the previously reported data, we observed substantial (up to ~90%) cell death with the unmodified TadA8e, which was alleviated following transfection with the TadA8e(V28R) mutant (**Supplementary Fig. 6**). The generation of TadA8e(V28R) enabled us to produce sufficient AAV titres for subsequent *in vivo* experiments. We then injected neonatal subjects (postnatal P1) with *Mt-Atp6* H-strand TadA8e(V28R) AAV9 with either DddAtox(E1357A) or BspD61(C) AAV9 via temporal vein injection at 5×10^{11} vg per monomer per animal (**Fig. 3a**). Upon sacrificing the animals at 4-weeks post-injection, we confirmed successful AAV delivery

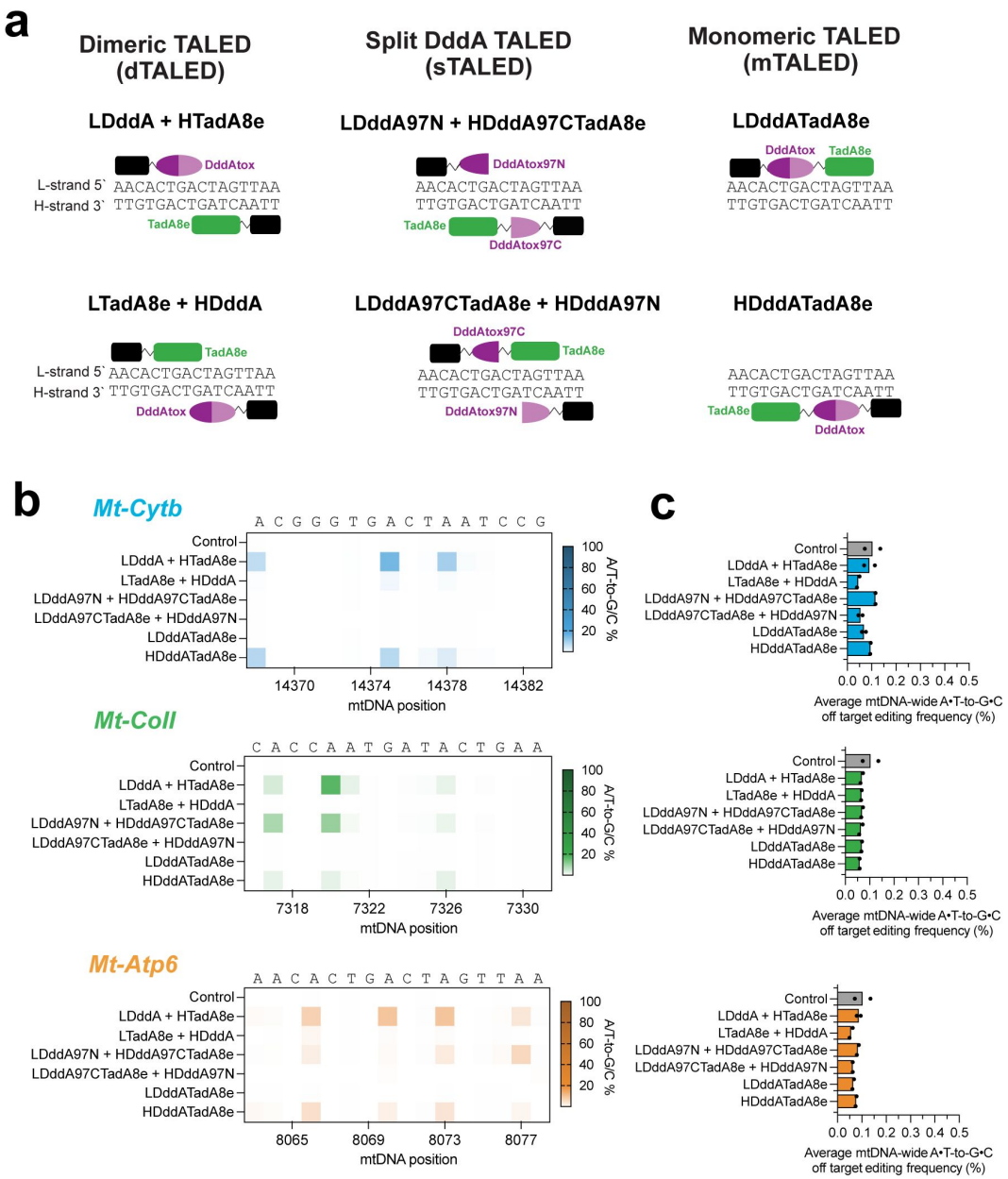

Fig. 1

Mitochondrial adenine base editing by TALED in cultured mouse cells.

a Schematic overview of the TALED adenine base editor architectures tested. The TadA8e enzyme is responsible for A:T to G:C editing, whilst DddAtox and Nt.BspD61(C) make the DNA accessible for enzyme activity. Black boxes indicate MTS and DNA binding elements. For full schematic see **Supplementary Fig. 1. b** On-target editing percentage values calculated by next generation sequencing of the six adenine base editor combinations targeted to the *Mt-Cytb*, *Mt-CoII* and *Mt-Atp6* genes using dTALED, sTALED and mTALED. Sequence and mouse mtDNA position is indicated. n = 2. **c** Average mtDNA-wide off-target editing frequency values calculated by next generation sequencing of the adenine base editor combinations targeted to the *Mt-Cytb*, *Mt-CoII* and *Mt-Atp6* genes from b. n = 2.

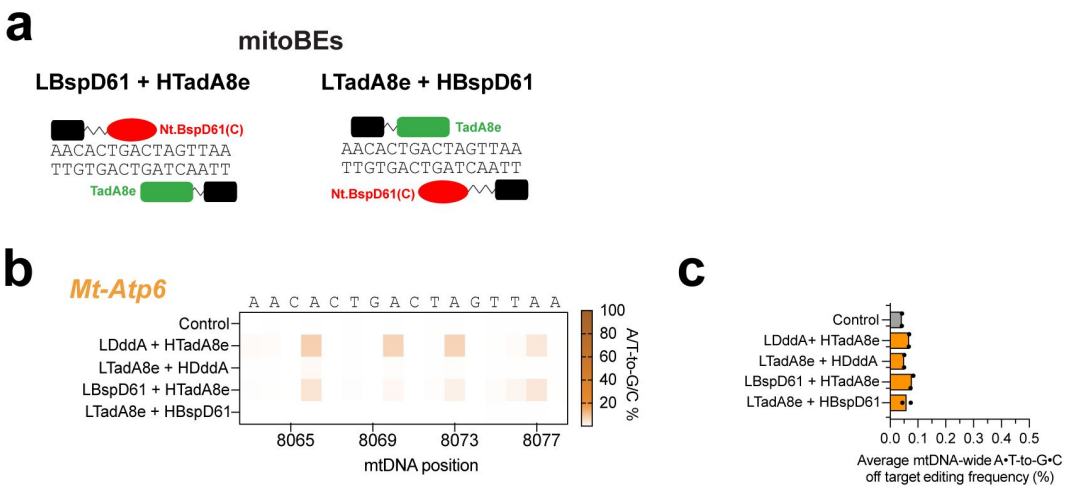

Fig. 2.

Mitochondrial adenine base editing by mitoBE in cultured mouse cells.

a Schematic overview of the mitoBE adenine base editor architectures tested. The TadA8e enzyme is responsible for A:T to G:C editing, while Nt.BspD61(C) make the DNA accessible for editing activity. Black boxes indicate MTS and DNA binding elements. For full schematic see **Supplementary Fig. 1. b** On-target editing percentage values calculated by next generation sequencing of base editors targeted to *Mt-Atp6* gene using mitoBE, containing the Nt.BspD61(C) nickase. n = 2. **c** Average mtDNA-wide off-target editing frequency values from d. Multiple t test comparison performed.

through robust expression in mouse cardiac and skeletal muscle tissue (**Supplementary Fig. 7** and **8**). At this time-point we observed minimal editing of mtDNA in mouse heart, with NGS revealing up to 0.5% of A:T to G:C edits in 3 replicate mice (**Fig. 3b-c**). However, we did not detect any editing in either skeletal muscle or liver tissues, as compared to control animals (**Fig. 3b-c**). We did not detect any mtDNA-wide off-targets above background, which was consistent with the low levels of edits observed (**Fig. 3d**). We further did not observe any significant changes in mtDNA copy number in the AAV-treated mice as compared to the vehicle-injected controls (**Fig. 3e**). We also did not detect any changes in OXPHOS protein steady state levels (**Supplementary Fig. 9** and **10**). Taken together, these findings confirm that adenine base editing of mtDNA in vivo in post-mitotic tissues is feasible upon AAV delivery, but the observed levels are notably low after a 4-week exposure period.

Conclusions

In this study, we tested the effect of adenine base editors first in cells using our TALEs targeted to *Mt-CytB*, *Mt-CoII* and *Mt-Atp6* and confirmed editing within the target window. We then tested the effect of *Mt-Atp6* adenine base editors in mice using AAV delivery to neonate mice and observed negligible editing in mouse hearts, with no editing in other tissues. In comparable experimental conditions, TALE-based DdCBE and ZF-DdCBEs installed up to 30% and 50% of C:G to T:A edits, respectively [15], [16]. Considering the limited editing efficiency and the absence of single-nucleotide specificity within the editing window, current adenine base editors need further optimization to become a valuable tool for generating or correcting pathogenic *in vivo* point mutations associated with mitochondrial diseases.

Data availability

The data supporting the findings of this study are available within the paper and its supplementary information files, apart from proprietary scripts which are available upon request by contacting the authors. The NGS files generated in this study have been deposited in GEO: GSE276406: Source data are provided with this paper. The materials used in this study are available upon request from M.M.

Supplementary material

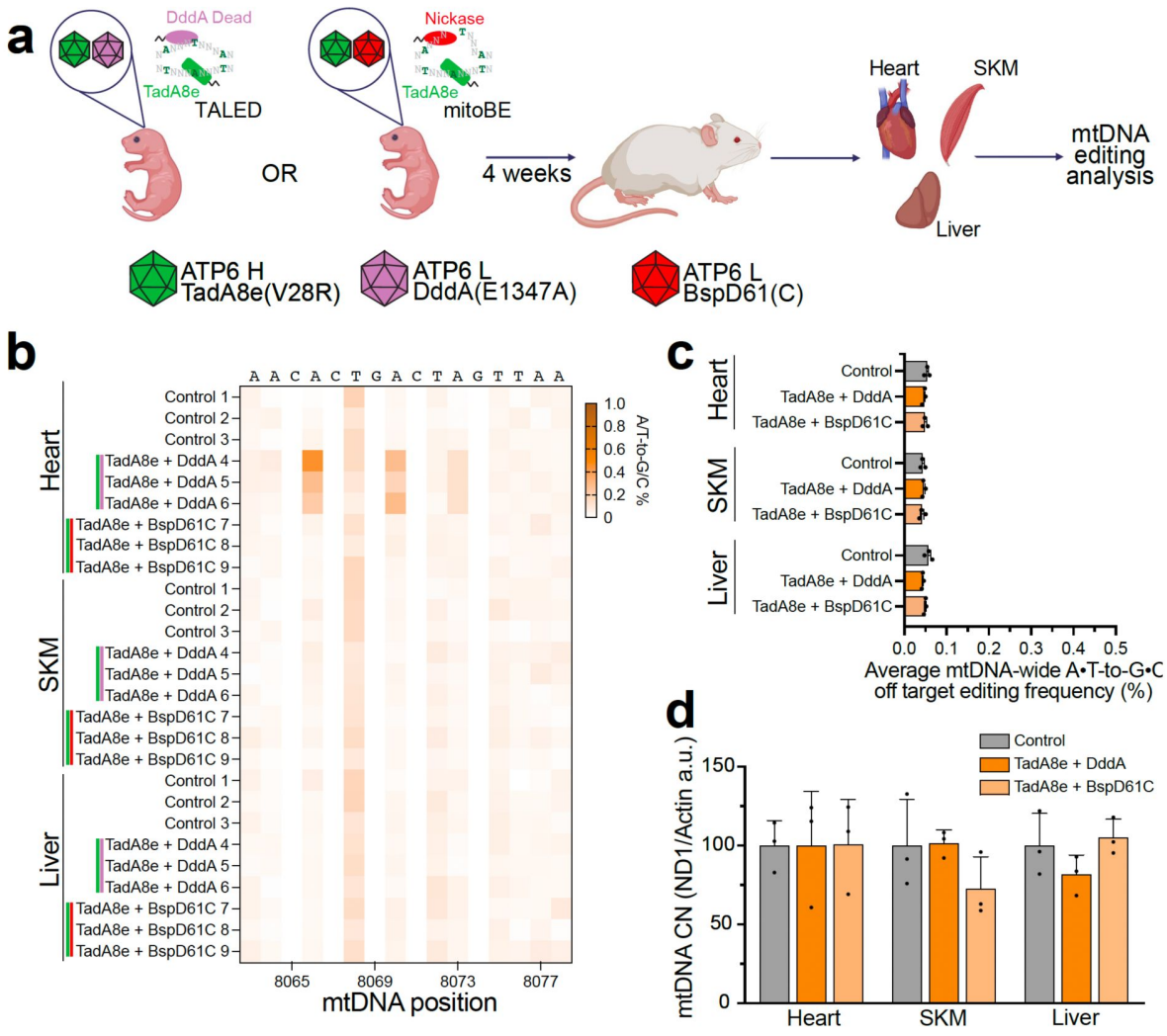

Fig. 3

In vivo mouse mtDNA editing using adenine base editors.

a Scheme of *in vivo* experiments with neonatal mice. TadA8e(V28R), DddAtox and BspD61(C) were encoded in separate AAV genomes, encapsidated in AAV9 then each pair (TadA8e(V28R) + DddAtox or TadA8e(V28R) + BspD61(C)) was imultaneously administered by temporal vein injection at 5×10^{11} vg/mouse of each monomer. Animals were sacrificed 4-weeks post-injection and their heart, skeletal muscle and liver tissues were examined for mtDNA editing. **b** On-target editing percentage values calculated by next generation sequencing of mouse tissues analysed following adenine base editor AAV delivery to the *Mt-Atp6* gene. Sequence and mouse mtDNA position is indicated. **c** Average mtDNA-wide off-target editing frequency values calculated by next generation sequencing from mice in b. Bars represent the mean and error bars represent ± SEM (n = 3). **d** Real-Time qPCR relative quantification of mtDNA copy number (CN) in 4-week-old mouse tissues following adenine base editor AAV delivery. Bars represent the mean and error bars represent ± SEM (n = 3). Multiple t test comparison performed.

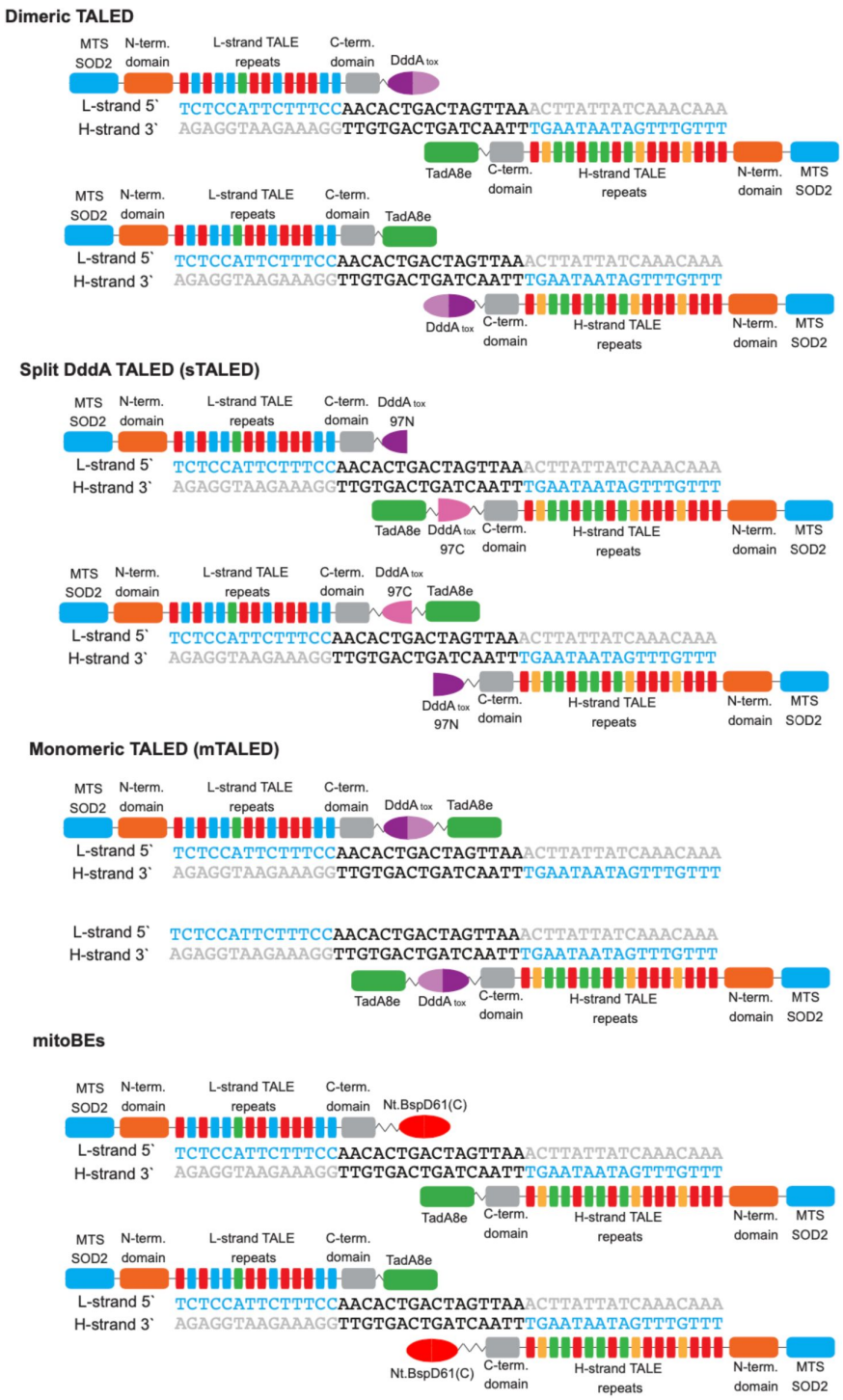

Supplementary Figure 1

Strategies for adenine base editing.

Schematics showing the four main methods used for adenine base editing in mitochondria. **Dimeric TALED (dTALED)** uses a TALE-binding mtDNA sequence specific protein attached to the catalytically dead DddAtox (for DNA unwinding) on one monomer, and the TadA8e adenine deaminase to the monomer binding the opposite mtDNA strand. **Split DddA TALED (sTALED)** which uses the G1397 split of the DddAtox attached to two TALED monomers, alongside the TadA8e. **Monomeric TALED (mTALED)** which contains only one sequence specific TALE protein attached to both the DddAtox and the TadA8e. Dimeric **mitoBEs** use nickase enzyme BspD61(C) to allow for single stranded activity of TadA8e.

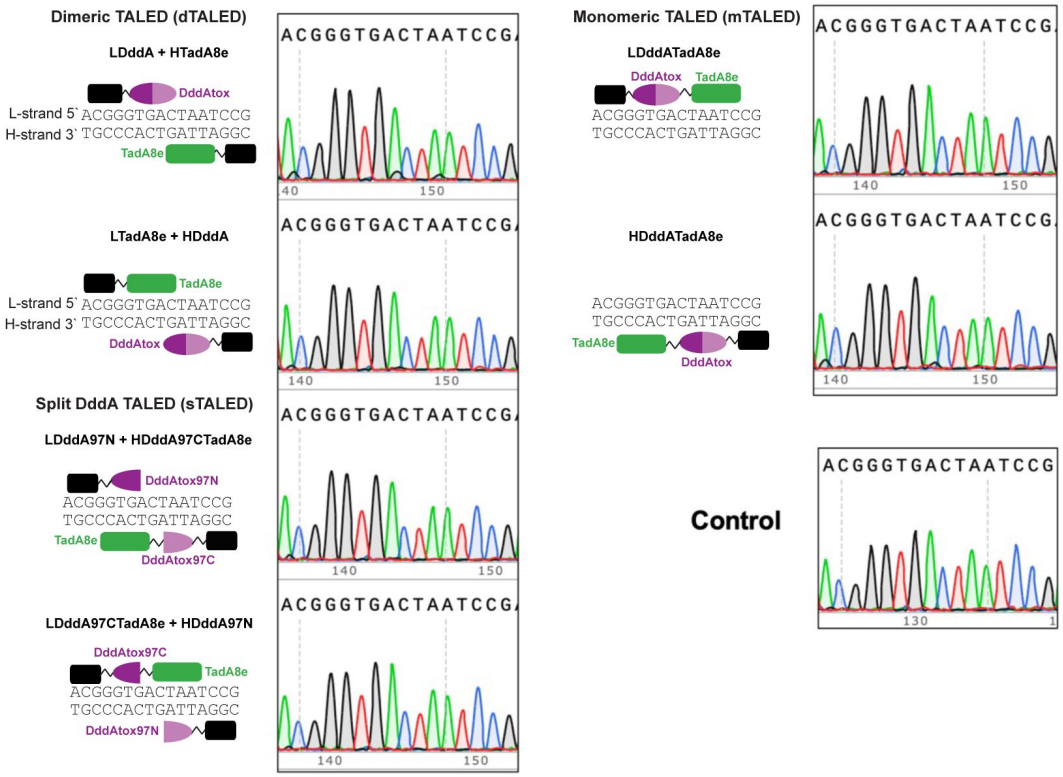

Supplementary Figure 2

Adenine base editing of *Mt-Cytb*.

Sanger sequencing traces of the six adenine base editor combinations targeted to the *Mt-Cytb* gene. Only the on-target editing window is shown.

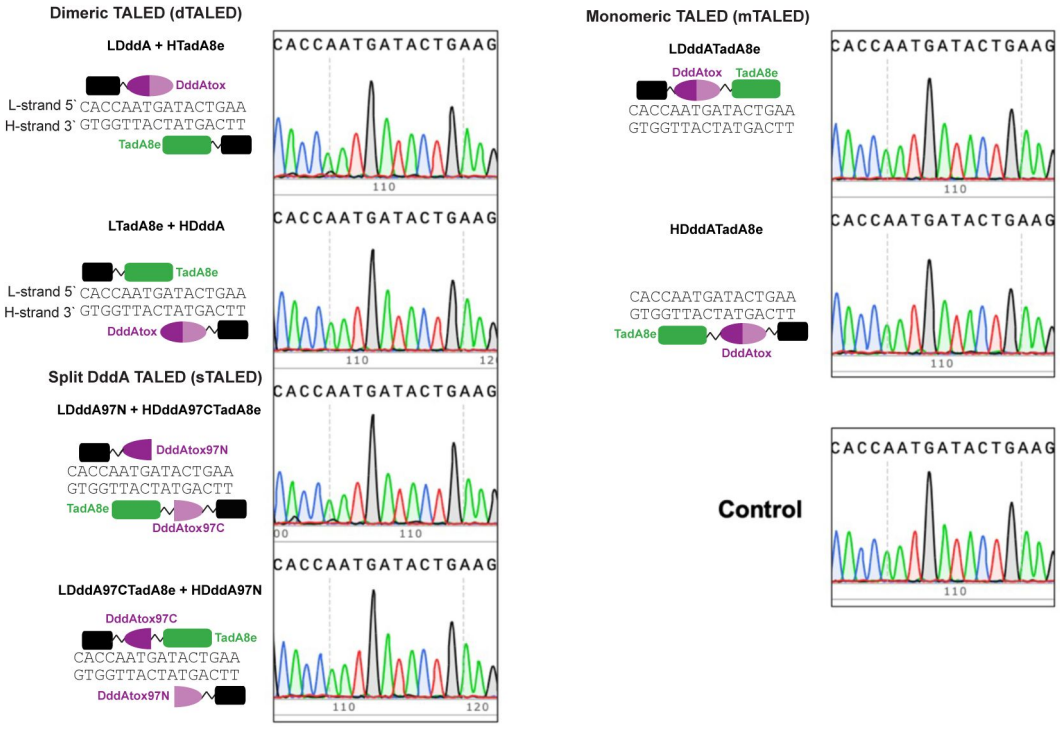

Supplementary Figure 3

Adenine base editing of *Mt-CoII*.

Sanger sequencing traces of the six adenine base editor combinations targeted to the *Mt-CoII* gene. Only the on-target editing window is shown.

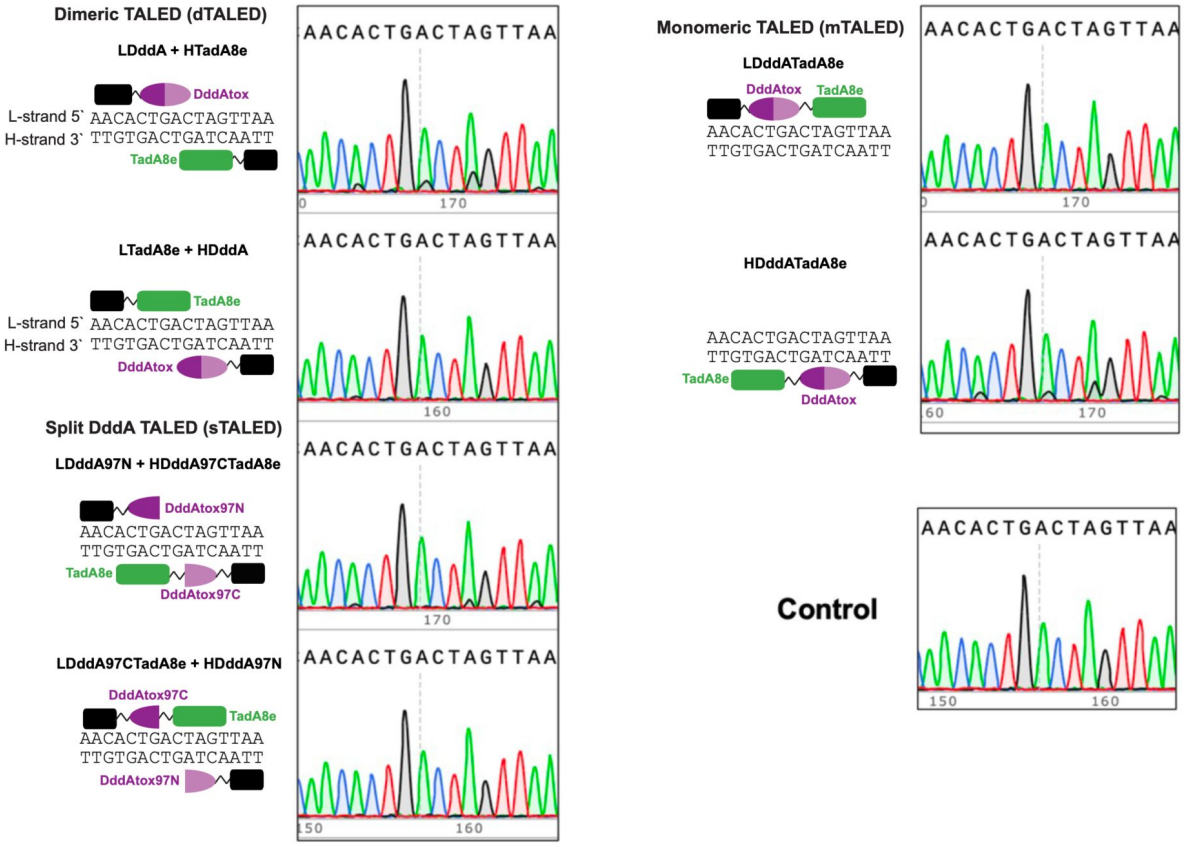

Supplementary Figure 4

Adenine base editing of *Mt-Atp6*.

Sanger sequencing traces of the six adenine base editor combinations targeted to the *Mt-Atp6* gene. Only the on-target editing window is shown.

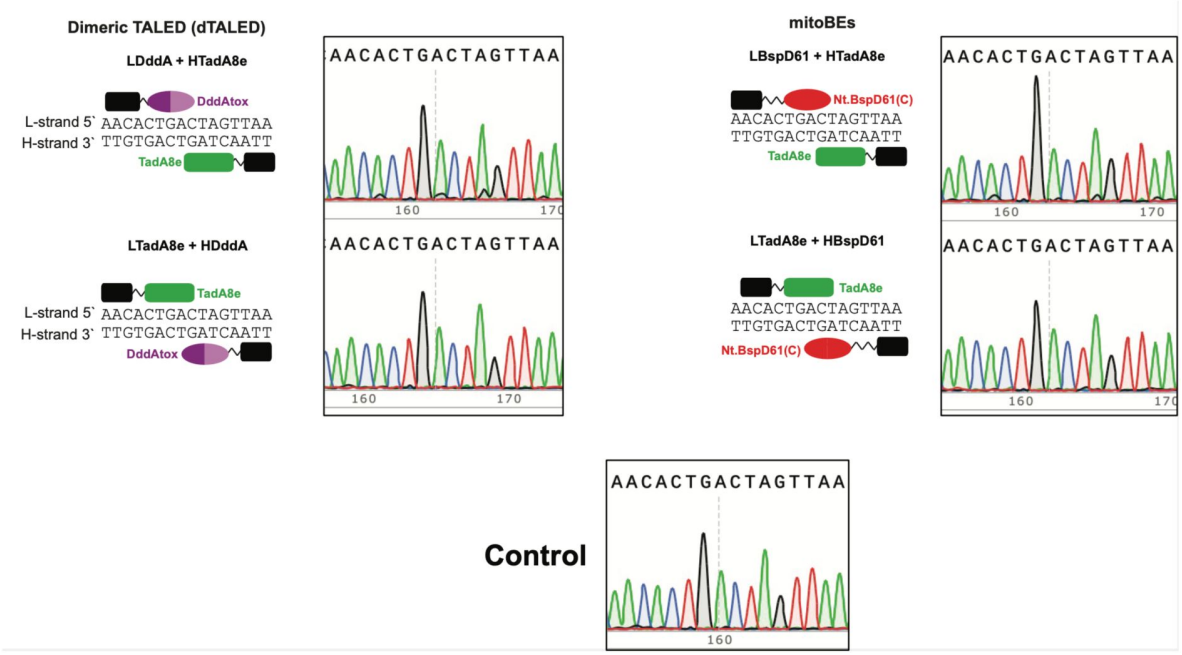

Supplementary Figure 5

Adenine base editing of *Mt-Atp6* by mitoBEs.

Sanger sequencing traces for the two mitoBE combinations targeting to the *Mt-Atp6* gene, compared to dTALED editing directed to the same gene. Only the on-target editing window is shown.

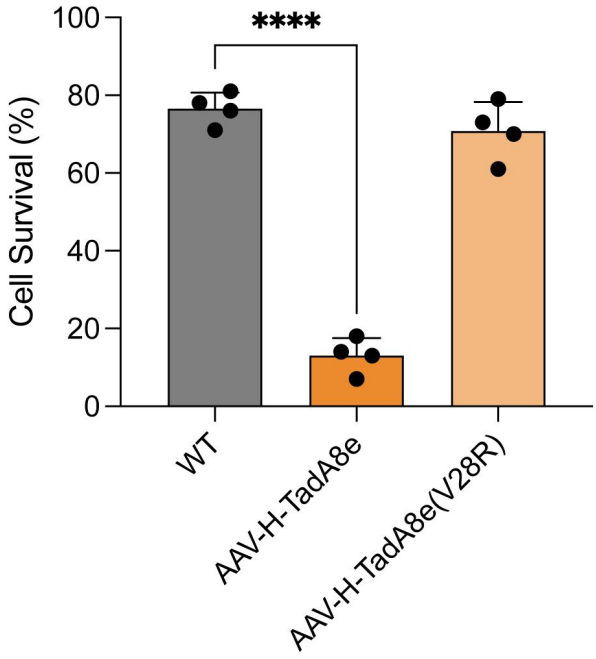

Supplementary Figure 6

Cell survival following transfection with AAV plasmids encoding TadA8e variants.

Cell survival percentage calculated using Countess Automated Cell Counter following 4 days post transfection of AAV plasmids spiked with empty GFP plasmid and sorting for enrichment. n = 4 biological replicates. Error bars indicate ±SEM Statistical significance was calculated from a one-tailed Student's t test **** P-value < 0.0001.

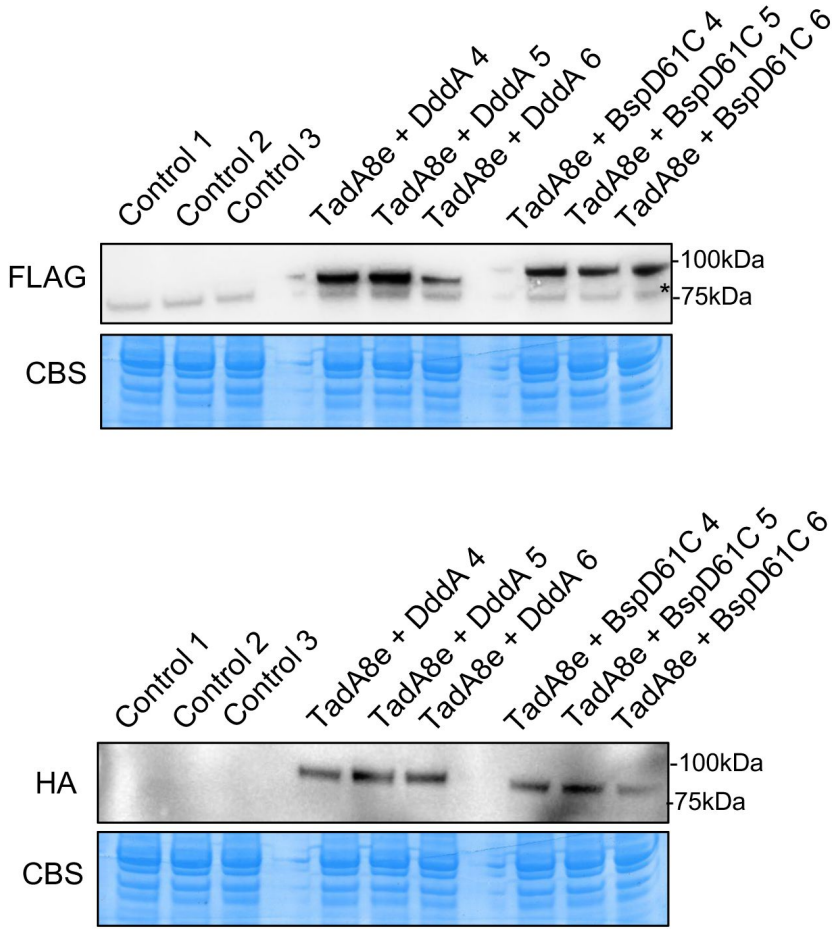

Supplementary Figure 7

Delivery of adenine base editor AAVs to mouse skeletal muscle.

Western blot analysis of the levels of FLAG-tagged AAV DddA or BspD61C (L) and HA-tagged AAV TadA8e (H) in skeletal muscle (quadriceps) of mice at 4 weeks post-injection. Coomassie Brilliant Blue (CBB) was used as loading control. * indicates a non-specific band detected by the anti-FLAG antibody.

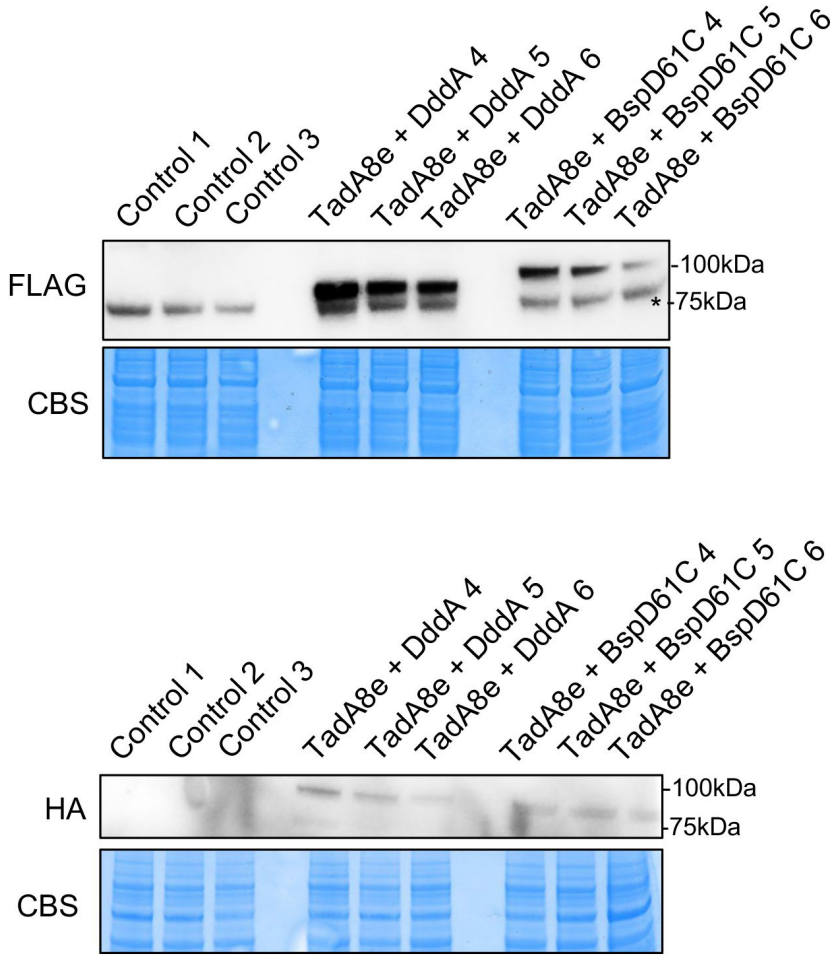

Supplementary Figure 8

Delivery of adenine base editor AAVs to mouse heart.

Western blot analysis of the levels of FLAG-tagged AAV DddA or BspD61C (L) and HA-tagged AAV TadA8e (H) in heart of mice at 4 weeks post-injection. Coomassie Brilliant Blue (CBB) was used as loading control. * indicates a non-specific band detected by the anti-FLAG antibody.

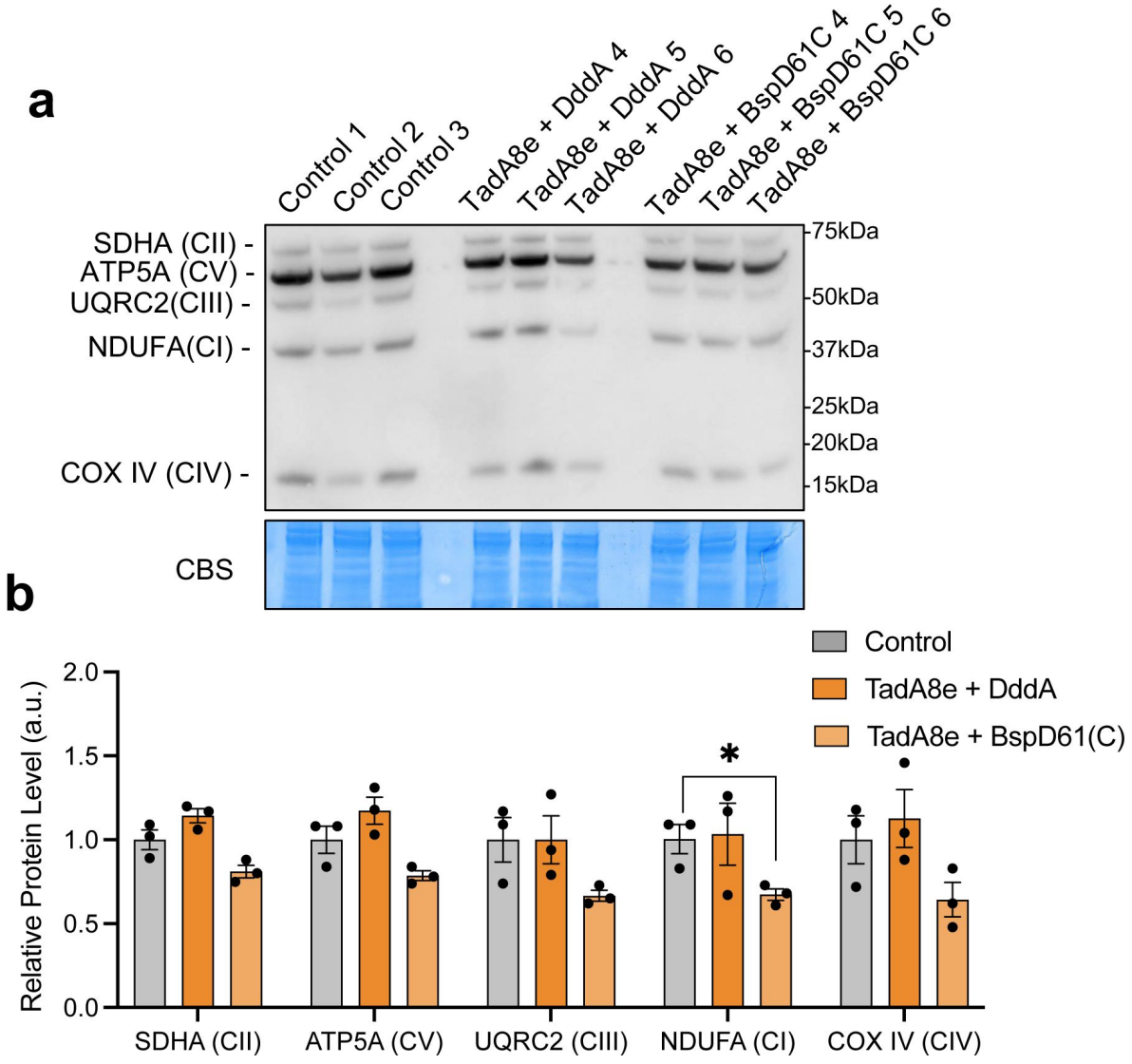

Supplementary Figure 9

Assessment of OXPHOS complex levels in skeletal muscle following adenine base editor AAV delivery.

a Western blot analysis of steady-state levels of components of OXPHOS in skeletal muscle of 4-week old control mice, mice injected with AAVs for TadA8e + DddA or TadA8e + BspD61(C). Coomassie Brilliant Blue (CBB) was used as loading control. **b** The western blots from a quantified using ImageJ. Error bars indicate ±SEM. Multiple t test comparison performed. *p<0.05.

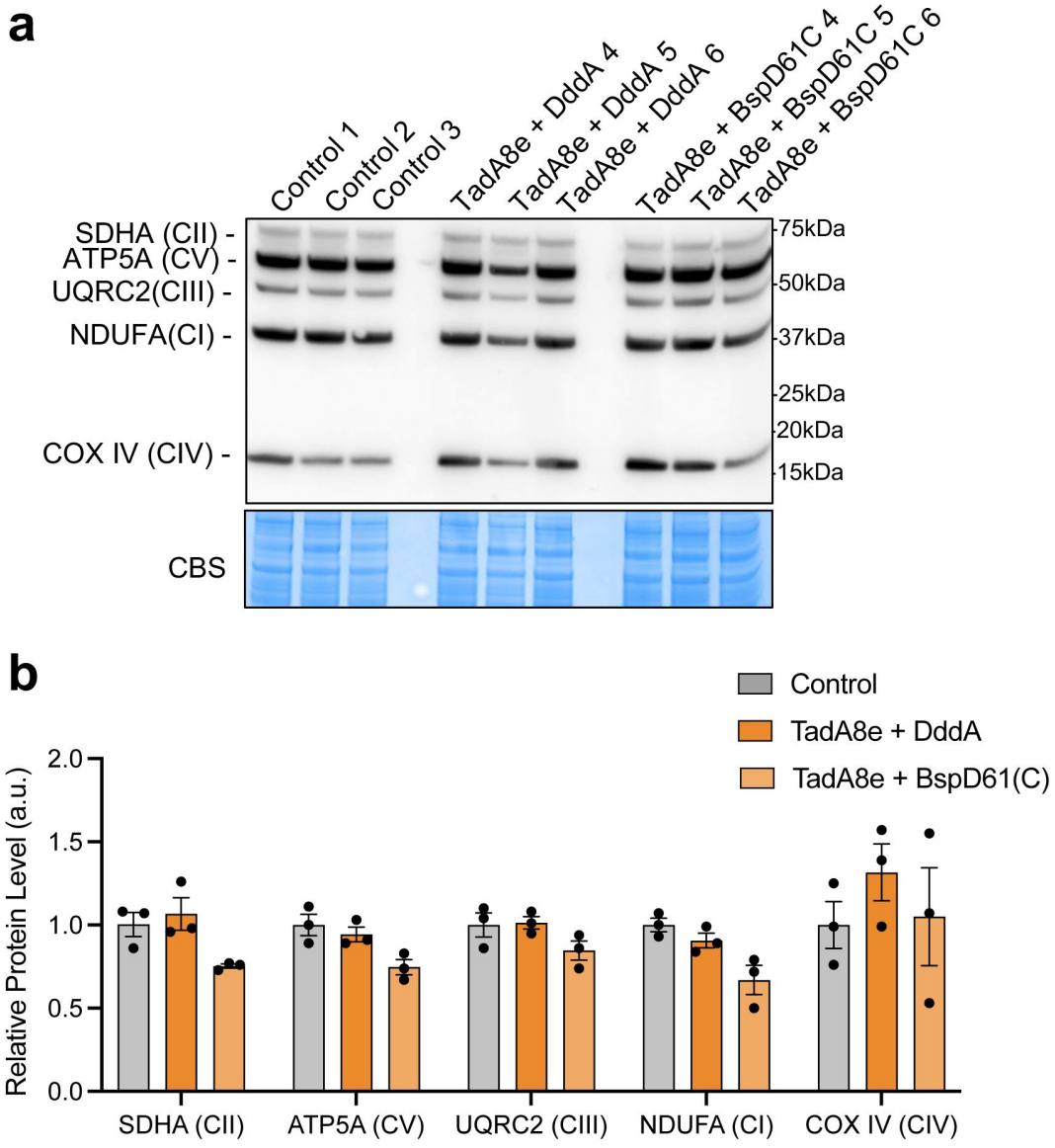

Supplementary Figure 10

Assessment of OXPHOS complex levels in heart following adenine base editor AAV delivery.

A Western blot analysis of steady-state levels of components of OXPHOS in heart of 4-week old control mice, mice injected with AAVs for TadA8e + DddA or TadA8e + BspD61(C). Coomassie Brilliant Blue (CBB) was used as loading control. **b** The western blots from a quantified using ImageJ. Error bars indicate ± SEM. Multiple t test comparison performed.

Acknowledgements

We would like to acknowledge the members of the Mitochondrial Genetics Group (MRC-MBU, University of Cambridge) for useful discussion during the course of this research. We would also like to thank the CIMR Flow facility for their support in this work.

Additional information

Funding

This work was supported by core funding from UKRI Medical Research Council UK (MRC) (MC_UU_00028/3), the UKRI MRC award MC_PC_21046 to the National Mouse Genetics Network Mitochondria Cluster (MitoCluster), AFM-Téléthon (#24237) and a research grant from the CureMito Foundation. P.S.-P. is additionally supported by The Champ Foundation.

Authors' contributions

C.D.M., P.S.-P. and M.M. planned and designed experiments; C.D.M. performed most of the experiments; L.V.H. analysed the NGS experiments; L.L.G. was involved in the NGS experiments, P.S.-P. performed the AAV in vivo experiments; K.T. managed the animal work. C.D.M., P.S.-P. and M.M. drafted the manuscript. P.S.-P. and M.M. supervised the study and acquired funds. All authors revised the manuscript.

References

[1] Russell O. M., Gorman G. S., Lightowlers R. N., Turnbull D. M. 2020) **Mitochondrial Diseases: Hope for the Future** *Cell* **181**:168 https://doi.org/10.1016/j.cell.2020.02.051

[2] Silva-Pinheiro P., Minczuk M. 2022) **The potential of mitochondrial genome engineering** *Nature Reviews Genetics* Nature Research **23**:199–214 https://doi.org/10.1038/s41576-021-00432-x

[3] Gammage P. A., Rorbach J., Vincent A. I., Rebar E. J., Minczuk M. 2014) **Mitochondrially targeted ZFNs for selective degradation of pathogenic mitochondrial genomes bearing large-scale deletions or point mutations** *EMBO Mol Med* **6**:458–466 https://doi.org/10.1002/emmm.201303672

[4] Gammage P. A., et al. 2016) **Near-complete elimination of mutant mtDNA by iterative or dynamic dose-controlled treatment with mtZFNs** *Nucleic Acids Res* **44**:7804–7816 https://doi.org/10.1093/nar/gkw676

[5] Bacman S. R., Williams S. L., Pinto M., Peralta S., Moraes C. T. 2013) **Specific elimination of mutant mitochondrial genomes in patient–derived cells by mitoTALENs** *Nat Med* **19** https://doi.org/10.1038/NM.3261

[6] Alexeyev M. F., Venediktova N., Pastukh V., Shokolenko I., Bonilla G., Wilson G. L. 2008) **Selective elimination of mutant mitochondrial genomes as therapeutic strategy for the treatment of NARP and MILS syndromes** *Gene Ther* **15**:516–523 https://doi.org/10.1038/GT.2008.11

[7] Zekonyte U., et al. 2021) **Mitochondrial targeted meganuclease as a platform to eliminate mutant mtDNA in vivo** *Nat Commun* **12** https://doi.org/10.1038/s41467-021-23561-7

[8] Mok B., et al. 2020) **A bacterial cytidine deaminase toxin enables CRISPR-free mitochondrial base editing** *Nature* https://doi.org/10.1038/s41586-020-2477-4

[9] Silva-Pinheiro P., et al. 2022) **A library of base editors for the precise ablation of all protein-coding genes in the mouse mitochondrial genome** *Nat Biomed Eng* https://doi.org/10.1038/s41551-022-00968-1

[10] Tan B. G., et al. 2022) **The human mitochondrial genome contains a second light strand promoter** *Mol Cell* https://doi.org/10.1016/j.molcel.2022.08.011

[11] Guo J., et al. 2021) **Precision modeling of mitochondrial diseases in zebrafish via DdCBE-mediated mtDNA base editing** *Cell Discovery* **7**:1–5 https://doi.org/10.1038/s41421-021-00307-9

[12] Sabharwal A., et al. 2021) **The FusX TALE Base Editor (FusXTBE) for Rapid Mitochondrial DNA Programming of Human Cells In Vitro and Zebrafish Disease Models In Vivo** *Crispr J* **4**:799–821 https://doi.org/10.1089/CRISPR.2021.0061

[13] Qi X., et al. 2021) **Precision modeling of mitochondrial disease in rats via DdCBE-mediated mtDNA editing** *Cell Discovery* Springer Nature **7** https://doi.org/10.1038/s41421-021-00325-7

[14] Lee H., et al. 2021) **Mitochondrial DNA editing in mice with DddA-TALE fusion deaminases** *Nature Communications* **12** https://doi.org/10.1038/s41467-021-21464-1

[15] Silva-Pinheiro P., Nash P. A., Van Haute L., Mutti C. D., Turner K., Minczuk M. 2022) **In vivo mitochondrial base editing via adeno-associated viral delivery to mouse post-mitotic tissue** *Nat Commun* **13** https://doi.org/10.1038/s41467-022-28358-w

[16] Willis J. C. W., Silva-Pinheiro P., Widdup L., Minczuk M., Liu D. R. 2022) **Compact zinc finger base editors that edit mitochondrial or nuclear DNA in vitro and in vivo** *Nat Commun* **13** https://doi.org/10.1038/s41467-022-34784-7

[17] Lim K., Cho S. I., Kim J. S. 2022) **Nuclear and mitochondrial DNA editing in human cells with zinc finger deaminases** *Nat Commun* **13** https://doi.org/10.1038/s41467-022-27962-0

[18] Mok B. Y., Kotrys A. V, Raguram A., Huang T. P., Mootha V. K., Liu D. R. 2022) **CRISPR-free base editors with enhanced activity and expanded targeting scope in mitochondrial and nuclear DNA** *Nat Biotechnol* https://doi.org/10.1038/s41587-022-01256-8

[19] Lee S., et al. 2022) **Enhanced mitochondrial DNA editing in mice using nuclear-exported TALE-linked deaminases and nucleases** *Genome Biol* **23** https://doi.org/10.1186/s13059-022-02782-z

[20] Sun H., et al. 2023) **Developing mitochondrial base editors with diverse context compatibility and high fidelity via saturated spacer library** *Nat Commun* **14** https://doi.org/10.1038/s41467-023-42359-3

[21] Cho S.-I., et al. 2022) **Targeted A-to-G base editing in human mitochondrial DNA with programmable deaminases** *Cell* https://doi.org/10.1016/j.cell.2022.03.039

[22] Yi Z., et al. 2023) **Strand-selective base editing of human mitochondrial DNA using mitoBEs** *Nat Biotechnol* https://doi.org/10.1038/s41587-023-01791-y

[23] Cho S. I., et al. 2024) **Engineering TALE-linked deaminases to facilitate precision adenine base editing in mitochondrial DNA** *Cell* **187**:95–109 https://doi.org/10.1016/j.cell.2023.11.035

[24] Gammage P. A., et al. 2018) **Genome editing in mitochondria corrects a pathogenic mtDNA mutation in vivo** *Nat Med* **24**:1691–1695 https://doi.org/10.1038/s41591-018-0165-9

Author information

Christian D Mutti
MRC Mitochondrial Biology Unit, University of Cambridge, Cambridge, United Kingdom

Lindsey Van Haute
MRC Mitochondrial Biology Unit, University of Cambridge, Cambridge, United Kingdom

Lucia Luengo-Gutierrez
MRC Mitochondrial Biology Unit, University of Cambridge, Cambridge, United Kingdom

Keira Turner
MRC Mitochondrial Biology Unit, University of Cambridge, Cambridge, United Kingdom

Pedro Silva-Pinheiro
MRC Mitochondrial Biology Unit, University of Cambridge, Cambridge, United Kingdom

For correspondence: pfdsp2@mrc-mbu.cam.ac.uk

Michal Minczuk
MRC Mitochondrial Biology Unit, University of Cambridge, Cambridge, United Kingdom, Department of Clinical Neurosciences, University of Cambridge, Cambridge, United Kingdom
ORCID iD: 0000-0001-8242-1420

For correspondence: michal.minczuk@mrc-mbu.cam.ac.uk

Editors

Reviewing Editor
Stephen Ekker
Mayo Clinic, Rochester, United States of America

Senior Editor
Didier Stainier
Max Planck Institute for Heart and Lung Research, Bad Nauheim, Germany

Reviewer #1 (Public review):

Summary:

This study represents an incremental step toward mitochondrial DNA editing but raises several concerns regarding its impact and broader applicability. The reported in vitro editing efficiency of 17% in mitotic cells, with non-specific editing across multiple A:T sites, offers limited improvement over prior technologies like DdCBE. Editing efficiency for the Mt-Atp6 gene was even lower (~4%), rendering it unlikely to produce functional changes relevant to mitochondrial function or bioenergetics.

While the modified TadA8e(V28R) mutant alleviated toxicity and enabled sufficient AAV production for in vivo experiments, the low in vivo editing efficiency (~4%) after 4 weeks was disappointing and unlikely to be biologically meaningful. Furthermore, the use of P1 postnatal tissues, which are still developing, raises questions about their suitability as models for postmitotic tissues, especially since the brain - a key organ affected by mitochondrial diseases - was excluded from the analysis.

Despite demonstrating feasibility for mitochondrial adenine base editing, the study highlights significant limitations, underscoring the need for further optimization. The reviewer also suggests adopting clearer terminology, such as "pathological variant" instead of "mutation," to enhance precision.

Strengths:

The study demonstrates the feasibility of adenine base editing in mitochondrial DNA, marking a step forward in expanding mitochondrial genome engineering capabilities. A notable strength is the development of a modified TadA8e(V28R) mutant, which successfully mitigated toxicity and enabled sufficient AAV production for in vivo experiments. This

technical advancement addresses a key challenge in mitochondrial gene editing and provides a foundation for improving delivery methods and reducing off-target effects.

Additionally, the study highlights the potential for targeted mitochondrial DNA modifications using optimized TALEs, achieving A:T to G:C conversions in multiple genes. While the in vitro editing efficiency remains modest, the approach represents an important proof-of-concept for potentially advancing mitochondrial editing technologies, particularly in the context of addressing pathological variants.

Weaknesses:

The major weaknesses of the study center around its low editing efficiency, both in vitro and in vivo. In vitro editing achieved only 17% efficiency in mitotic cells, while the efficiency for the Mt-Atp6 gene was even lower, around 4%. This level of editing is unlikely to produce meaningful functional or biological changes, particularly in cells with pathological mtDNA variants. Similarly, in vivo, editing efficiency after a 4-week exposure period remained at approximately 4%, which is insufficient to support claims of effective mitochondrial genome editing. Another significant limitation is the lack of editing specificity, as observed changes occurred at multiple A:T sites within and across the editing window rather than being confined to a single position, raising concerns about precision and off-target effects.

The use of P1 postnatal mouse tissues also raises questions about the relevance of the model, as these tissues are still undergoing development and may not truly reflect postmitotic states. This casts doubt on whether the findings are transferable to mature tissues, such as the adult brain, which is frequently affected by mitochondrial diseases. Furthermore, the exclusion of brain tissue from the analysis limits the study's applicability to neurological disorders, a key area of mitochondrial disease research. The rationale for excluding brain tissue is not addressed, leaving an important gap in the study's scope.

The findings also lack novelty, as the reported low efficiency and lack of specificity are consistent with previous studies, making it unclear whether this work represents a significant advancement over existing technologies.

Collectively, these weaknesses underscore the need for further optimization of the approach, improved targeting specificity, and validation in more relevant models to demonstrate therapeutic potential.

https://doi.org/10.7554/eLife.105080.1.sa1

Reviewer #2 (Public review):

The authors have demonstrated the use of adenine base editors delivered via adeno-associated viruses to introduce edits in the mitochondrial genome. The manuscript describes the methodology well, and the conclusions are aptly supported by the results. It highlights the potential of these base editors to model mtDNA variations in somatic tissues in animal models.

However, there are a few comments that need to be addressed:

(1) Limitations of the small sample size need to be explained clearly for the results described.

(2) It will be beneficial for the readers if some light is shed on the possible reasons why the efficiencies of adenine base editing are lower than those reported for published cytosine base editors to introduce edits in the mitochondrial DNA.

(3) The conclusion should more explicitly address the limitations and future directions on low editing efficiency and what can be possible optimization steps.

(4) In Figure 1, A-to-G editing for the genes Mt-Cytb, Mt-CoII, and Mt-Atp6 appears to be strand-specific for the different architectures of adenine base editors. Do authors have a possible hypothesis if one of the strands is more favorable to editing depending on where the TadA8 binds or is it random?

https://doi.org/10.7554/eLife.105080.1.sa0